

# Synthesis of Highly Stable Porous Metal-Iminodiacetic Acid Gels from a Novel IDA Compound

Wenjing Chen,<sup>a,b</sup> Yanhong Jiang,<sup>a</sup> Xuesong Ding,<sup>\*,b</sup> Chaoguo Yan,<sup>\*,a</sup> and Baohang Han<sup>\*,b</sup>

<sup>a</sup> College of Chemistry and Chemical Engineering, Yangzhou University, Yangzhou, Jiangsu 225002, China  
<sup>b</sup> CAS Key Laboratory of Nanosystem and Hierarchical Fabrication, CAS Center for Excellence in Nanoscience, National Center for Nanoscience and Technology, Beijing 100190, China

In this work, a novel and simple flexible aromatic multi-carboxylate compound *N,N'*-(4,4'-biphenylyl) iminodiacetic acid (BP-IDA) was synthesized, with which two new stable metal-IDA gels (denoted as MIG1 and MIG2) with three-dimensional network structures have been prepared successfully by employing Cr<sup>3+</sup> and Al<sup>3+</sup> as the metal ions, respectively. The rheological performance was investigated by means of dynamic rheology measurement. The morphology and microstructure were characterized by scanning electron microscopy, transmission electron microscopy, and X-ray diffraction technique. Nitrogen sorption isotherm measurement suggests that the MIG1 aerogel has considerable porosity with the Brunauer-Emmett-Teller specific surface area up to 760 m<sup>2</sup>·g<sup>-1</sup>. Owing to easy preparation, good stability, and three-dimensional network structure, the as-prepared metal-organic gels will possess potential applications in separation, catalysis, and drug delivery.

**Keywords** iminodiacetic acid, chromium(III) ion, aluminum(III) ion, metal-IDA gels, porosity

## Introduction

Metal-organic frameworks (MOFs), which consist of metal ions or clusters coordinated to rigid organic ligands to form periodic infinite network structures and crystalline materials, have been springing up and widely studied as a new type of porous materials in the past decades.<sup>[1]</sup> Owing to their unique structures, MOFs can be utilized in versatile applications such as adsorption,<sup>[2]</sup> ion exchange, molecular recognition, catalytic, and optical,<sup>[3]</sup> electrical, magnetic, chiral separation fields.<sup>[4]</sup> MOFs are commonly in the form of powdery crystal. To obtain a large size with a specific shape, the forming process through adhesive generally results in the decrease of specific surface area and the blockage of pores.<sup>[5]</sup> Therefore, it is still a huge challenge to process MOFs<sup>[6]</sup> into optimal shape in the industry. In recent years, supramolecular gels have attracted tremendous attentions as a class of multifunctional materials. Among them, the research on supramolecular gel construction using the concept of coordination polymer and introducing metal ions, called metal-organic gel, has just begun and aroused people's attention gradually due to its potential applications in optical, electrical, and catalysis fields.<sup>[7,8]</sup> The generation of metal-organic gels with three-dimensional (3D) network structures is mainly based on the coordination of metal ions and organic ligands, as well as some relatively weak non-co-

valent interactions, such as hydrogen bonding, van der Waals force, and π-π interaction.<sup>[9,10]</sup> Compared with MOFs, the metal-organic gels possess poor crystallinities and unclear structures, however, they still have the following advantages: (1) The reaction can proceed at a low temperature, some materials can be obtained at room temperature; (2) the reaction time is shorter and solvent quantity is less; (3) reaction solvent is cheap and with low toxicity, the reaction can proceed in ethanol, water, *N,N'*-dimethylformamide (DMF), or the mixture of them; (4) the easily obtained desired shapes of the gels by utilizing various shapes of reaction containers make them more suitable for industrialized and commercial applications. Due to above points, metal-organic gels have amounts of potential applications in catalysis,<sup>[11]</sup> sensing,<sup>[12]</sup> anion recognition,<sup>[13]</sup> photophysics,<sup>[14,15]</sup> vapor adsorption,<sup>[16]</sup> separation technologies, electrochemical detection,<sup>[17]</sup> etc. Conformationally flexible ligands with amide groups<sup>[18-20]</sup> have been often employed to design metal-organic gels because the formed networks are able to trap solvent molecules in their crystal lattices. However, because the structures of most ligands are complex with multi-step procedure, the synthesis and functional researches of metal-organic gels are still rarely reported up to date.

In this work, we design and synthesize a new flexible aromatic multi-carboxylate compound *N,N'*-(4,4'-biphenylyl) iminodiacetic acid (BP-IDA) in two steps

\* E-mail: hanbh@nanoctr.cn; egyan@yzu.edu.cn; dingxs@nanoctr.cn

Received March 29, 2016; accepted May 6, 2016; published online June 15, 2016.

Supporting information for this article is available on the WWW under <http://dx.doi.org/10.1002/cjoc.201600184> or from the author.

that is inspired by ethylene diamine tetraacetic acid (EDTA). Besides the considerations mentioned above about multi-carboxylate ligands, BP-IDA has its own remarkable features. Firstly, conformationally flexible ligands with auxiliary chemical interaction have often been employed to design coordination polymers<sup>[21–23]</sup> and metal-organic gels, and BP-IDA contains flexible multi-carboxylate structures coincidentally. As a polycarboxylic acid, BP-IDA is similar to EDTA. The nitrogen atom and two carboxylate groups of the iminodiacetate part can afford more abundant types of coordination architectures to chelate metal ions strongly.<sup>[24,25]</sup> Secondly, BP-IDA is more sensitive to chelate metal ions with the flexible methylene groups,<sup>[26]</sup> they can freely twist to meet the requirements of the coordination geometries of metal atoms,<sup>[27,28]</sup> and may induce metal clusters and link them into an extended framework with various coordination modes.<sup>[29]</sup> Thirdly, the introduced aromatic and carboxylate groups could offer additional sites for  $\pi$ - $\pi$  interaction and hydrogen bonding, respectively. These non-covalent interactions further consolidate the structures of coordination polymers.<sup>[6,30]</sup> Above all, BP-IDA with simple and flexible structure is very suitable as a ligand to produce metal-organic gels. These metal-organic gels are defined as metal-IDA gels (MIGs). We prepared two new stable metal-IDA gels successfully from the bridging ligand and Cr<sup>3+</sup> and Al<sup>3+</sup> as the metal ions,<sup>[31]</sup> and these gels have lots of potential applications owing to their 3D network structure, satisfactory strength, porosity, and stability.

## Experimental

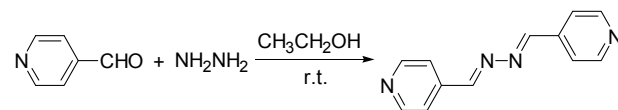
### Materials

Ethyl bromoacetate, potassium iodide, anhydrous potassium hydrogen phosphate, acetonitrile, petroleum ether, ethyl acetate, ethanol, sodium hydroxide, hydrochloric acid, hydrazine hydrate, *tert*-butanol, and *N,N'*-dimethylformamide (DMF) were purchased from Beijing Chemical Reagents Company and of analytical grade. Benzidine, pyridine-4-carboxaldehyde, chromic nitrate nonahydrate, and aluminum nitrate nonahydrate were purchased from Sigma-Aldrich. *N,N'*-Bis-pyridin-4-ylmethylene-hydrazine (4-bpmb) (Scheme 1),<sup>[15,32]</sup> *N,N'*-(4,4'-biphenyl)-iminodiacetic acid (BP-IDA) (Scheme 2)<sup>[33–35]</sup> were synthesized according to the reported procedures.

### Synthesis of *N,N'*-bis-pyridin-4-ylmethylene-hydrazine (4-bpmb)

Pyridine-4-ylmethylene-hydrazine (4.49 g, 40.00 mmol) was dissolved in 15 mL ethanol in a 25 mL round bottom flask, and then hydrazine hydrate (1.03 g, 21.00 mmol) was added slowly with vigorous stirring. After 15 min, the yellow precipitate appeared, 4-bpmb was obtained by filtration in 70% yield. <sup>1</sup>H NMR (400 MHz, CDCl<sub>3</sub>)  $\delta$ : 8.76 (s, 4H, ArH), 8.57 (s, 2H, CH<sub>2</sub>), 7.70 (s, 4H, ArH) (Figure S7, Supporting Information).

### Scheme 1 Synthesis of compound 4-bpmb



### Synthesis of *N,N'*-(4,4'-biphenyl)-diethyl iminodiacetate (BP-IDE)

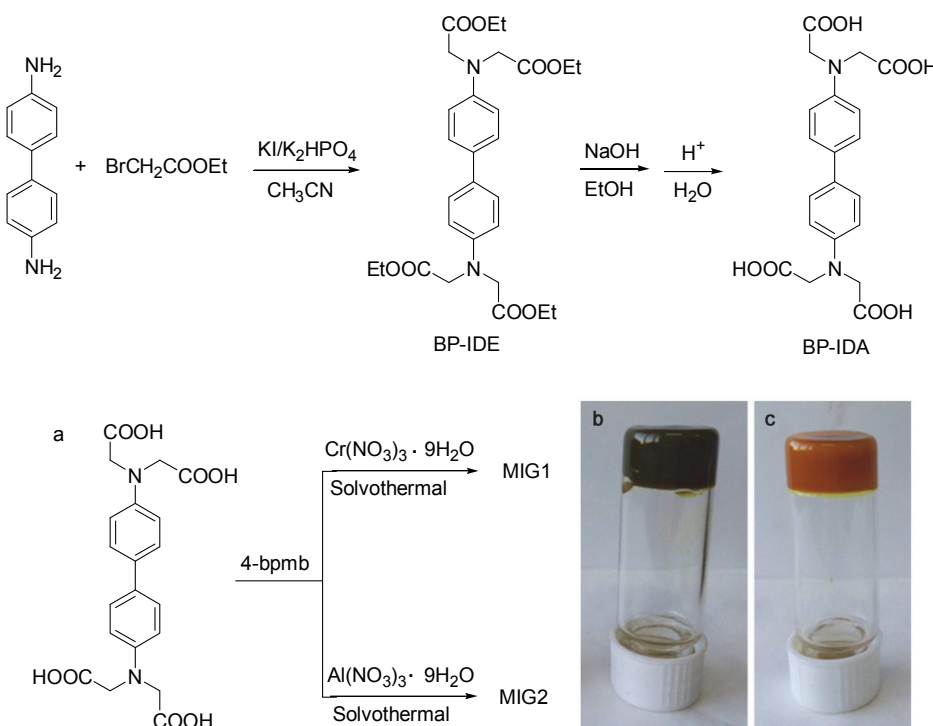
Benzidine (1.84 g, 10.00 mmol), KI (7.97 g, 48.00 mmol), and K<sub>2</sub>HPO<sub>4</sub> (8.30 g, 48.00 mmol) were added into a dry 250 mL round bottom flask and dissolved in 120 mL anhydrous acetonitrile and ethyl bromoacetate (4.86 mL, 44.00 mmol) under nitrogen atmosphere. The reaction mixture was heated to 80 °C and refluxed for 40 h, and then cooled to room temperature. The residue was removed by filtration, and the collected filtrate was concentrated under vacuum to obtain an oily product. The crude product was purified by silica chromatography using ethyl acetate/petroleum ether (1/2) as eluant, BP-IDE was obtained as gray solids in 63% yield (Scheme 1). <sup>1</sup>H NMR (400 MHz, CDCl<sub>3</sub>)  $\delta$ : 7.39 (d,  $J$ =8.0 Hz, 4H, ArH), 6.65 (d,  $J$ =8.0 Hz, 4H, ArH), 4.22 (dd,  $J$ =8.0 Hz, 8H, CH<sub>2</sub>), 4.16 (s, 8H, CH<sub>2</sub>), 1.28 (t,  $J$ =8.0 Hz, 12H, CH<sub>3</sub>); <sup>13</sup>C NMR (100 MHz, CDCl<sub>3</sub>)  $\delta$ : 171.0, 146.6, 131.1, 127.3, 112.9, 61.1, 53.6, 14.3. HRMS (ESI) calcd for C<sub>28</sub>H<sub>36</sub>N<sub>2</sub>NaO<sub>8</sub> ([M+Na]<sup>+</sup>) 551.2364, found 551.2373 (Figures S1–S3, Supporting Information).

### Synthesis of *N,N'*-(4,4'-biphenyl)-iminodiacetic acid (BP-IDA)

In a 100 mL round bottom flask, BP-IDE (2.64 g, 5.00 mmol) was dissolved in 50 mL ethanol, the reaction mixture was heated to 78 °C, aqueous NaOH solution (2.0 mol/L) was added slowly under heating until pH=8.0, the mixture was refluxed for 4 h. After cooling to room temperature, ethanol was removed to get brown solids. The sodium salt of BP-IDE was dissolved in H<sub>2</sub>O (30 mL) and acidified with diluted HCl solution until no further precipitate generated, finally the brown product BP-IDA was obtained by filtration in 86% yield (Scheme 1). <sup>1</sup>H NMR (400 MHz, DMSO-d<sub>6</sub>)  $\delta$ : 7.37 (d,  $J$ =8.0 Hz, 4H, ArH), 6.50 (d,  $J$ =8.0 Hz, 4H, ArH), 4.03 (s, 8H, CH<sub>2</sub>); <sup>13</sup>C NMR (100 MHz, DMSO-d<sub>6</sub>)  $\delta$ : 174.0, 146.3, 129.2, 126.8, 112.0, 55.7. HRMS (ESI) calcd for C<sub>20</sub>H<sub>19</sub>N<sub>2</sub>O<sub>8</sub> ([M-H]<sup>-</sup>) 415.1147, found 415.1158 (Figures S4–S6, Supporting Information).

### Preparation of MIG1 aerogel

BP-IDA (0.042 g, 0.10 mmol), 4-bpmb (0.042 g, 0.20 mmol), and Cr(NO<sub>3</sub>)<sub>3</sub>•9H<sub>2</sub>O (0.120 g, 0.30 mmol) in 2 mL DMF were sealed in a 10 mL Teflon-lined autoclave, then the suspension was subjected to ultrasonic treatment until a clear mixture was got. The reaction system was kept at 120 °C for 3 h, and then the MIG1 can be obtained (Figure 1). The blackgreen gel was washed with DMF to remove unreacted starting materials. Then, the wet gel was immersed in a large

**Scheme 2** Synthesis of compound BP-IDA**Figure 1** Synthesis of metal-IDA gels (a) and photographic images of MIG1 (b) and MIG2 (c) gels in DMF.

amount of *tert*-butanol thoroughly to exchange DMF. Finally the aerogel was obtained by freeze-drying under vacuum (less than 20 Pa) for 24 h. The product is named MIG1 aerogel. The preparation conditions were optimized through varying feeding ratios, temperatures, and concentrations, respectively (Tables S1–S4, Supporting Information).

### Preparation of MIG2 aerogel

The synthesis of MIG2 aerogel was similar to that of MIG1 aerogel, except that  $\text{Cr}(\text{NO}_3)_3 \cdot 9\text{H}_2\text{O}$  was replaced by  $\text{Al}(\text{NO}_3)_3 \cdot 9\text{H}_2\text{O}$  (Figure 1 and Table S5, Supporting Information).

### Instrumental characterization

$^1\text{H}$  NMR and  $^{13}\text{C}$  CP/MAS NMR spectra were collected by a Bruker Advance III 400 NMR spectrometer (Bruker, Germany). Infrared (IR) spectra were recorded in KBr pellets with a Spectrum One Fourier transform infrared (FT-IR) spectrometer (PerkinElmer Instruments Co. Ltd., U.S.A.). The IR sample was prepared by dispersing the solid in KBr and compressing the mixtures to form disks, and 16 scans were signal-averaged. Scanning electron microscopy (SEM) observations were carried out using a S-4800 microscope (Hitachi Ltd., Japan) at an accelerating voltage of 6.0 kV. Transmission electron microscopy (TEM) observations were carried out using a Tecnai G<sup>2</sup> S-TWIN microscope (FEI, U.S.A.) at an accelerating voltage of 200 kV. X-ray photoelectron spectroscopy (XPS) data were acquired with an ESCA-Lab220i-XL electron spectrometer (VG Scientific Ltd.,

U.K.) using 300 W Al  $\text{K}\alpha$  radiation. Thermogravimetric analysis (TGA) was performed on a Pyris Diamond thermogravimetric/differential thermal analyzer (PerkinElmer Instruments Co. Ltd., U.S.A.) by heating the samples at  $10\ ^\circ\text{C} \cdot \text{min}^{-1}$  to  $800\ ^\circ\text{C}$  under nitrogen atmosphere. Power X-ray diffraction (PXRD) patterns were measured from  $4^\circ$  to  $40^\circ$  by a Philips X'Pert PRO X-ray diffraction instrument (Philips, Netherlands). Nitrogen adsorption-desorption experimentation was conducted using a 3Flex surface characterization analyzer (Micromeritics, U.S.A.). The analysis was measured at 77 K, and the obtained nitrogen sorption isotherm was assessed to give pore properties such as specific surface area, pore size distribution, total pore volume, and so on. The rheological properties were tested by a MARS2 rheometer (HAKKE, Thermo Scientific, Germany) with 25 mm diameter parallel-plate geometry at  $25\ ^\circ\text{C}$ , the gap distance between two plates was fixed to 2 mm and the frequency sweep was in the range from 0.02 to 100  $\text{rad} \cdot \text{s}^{-1}$  at a fixed oscillatory strain of 1%.<sup>[36]</sup>

### Results and Discussion

IDA is well-known for a long time, which can coordinate to metal ions as a common multidentate ligand.<sup>[37]</sup> As a derivative of IDA, the obtained BP-IDA can also chelate metal ions by two IDA groups. According to the literature,<sup>[17]</sup> once the auxiliary *N*-donor ligand is introduced into the system, BP-IDA tends to form ideal tridentate mode with metal atoms through IDA, *N*-donor,

and solvent molecule.<sup>[18,21,38]</sup> In this work, gels were fabricated through simple mixing of BP-IDA, auxiliary ligand, and metal salt in DMF solution above 80 °C. It is rationalized that the mechanism underpinning the construction of metal-organic gel hybrid progresses in accordance with Figure 2, endorsed by theoretical inference and experimental observations. Different from most metal-organic gels,<sup>[39,40]</sup> the as-synthesized MIG1 and MIG2 are very stable when kept for more than several months under ambient environment (room temperature and pressure) without collapsing, and they can not be dissolved under heating. Meanwhile, the state of MIGs has no change to the external mechanical force due to their high strength.

Several preparation conditions have been changed (such as metal-BP-IDA ratio, temperature, and concentration) in order to obtain better and more stable network structures of MIGs. All the experiments are carried out in DMF due to the poor solubility of BP-IDA in other solvents, the ratio of 4-bpmb to BP-IDA is invariable (4-bpmb/BP-IDA=2/1). Firstly, because different metal-BP-IDA ratios are able to affect the 3D network structures of the gels, several groups of experiments are designed with different metal-BP-IDA ratios from 1 : 1 to 6 : 1. According to the structures and the specific surface area of MIG aerogels, metal/BP-IDA=3/1 is found to be the optimum proportion (Tables S1 and S4, Supporting Information). Secondly, the experiments are studied at six different temperatures from 70 to 160 °C (Tables S2 and S4, Supporting Information), owing to the temperature of reaction can influence the gelation time and the intensity of gels. Metal-IDA gels can be formed above 80 °C, and higher reaction temperature leads to shorter gelation time and stronger structure. It is

found that 150 °C is the optimum temperature. So far, lots of gels that are sensitive to temperature have been reported, and gel-to-sol transition was observed upon heating and the solutions reverted to gel upon cooling.<sup>[41]</sup> Interestingly, metal-IDA gels synthesized can maintain their gel state and strength at high temperature for several days, and these highly stable gels were rarely reported in previous literature. Thirdly, the solution concentrations could influence the strength of gels, and obviously concentrated solution led to faster and stronger gel formation than diluted one. The solutions with various concentrations from 0.025 to 0.100 mol·L<sup>-1</sup> (the concentration is based on BP-IDA) are used (Tables S3 and S4, Supporting Information). Compared with the gel formed under 0.100 and 0.025 mol·L<sup>-1</sup>, the concentration of 0.05 mol·L<sup>-1</sup> is the optimum proportion for the gel strength and the aerogel porosity. Taking together, the optimum metal-IDA gel preparation condition is the ratio of metal/BP-IDA/4-bpmb=3/1/2, temperature of 150 °C, and concentration of 0.05 mol·L<sup>-1</sup>.

The viscoelastic nature of these gels was confirmed by rheological measurements. Firstly, oscillatory amplitude sweep was performed on the sample in order to choose the strain at which the dynamic frequency sweep is required to be carried out. From the frequency sweep measurements, a strain of 1% was determined to test the storage modulus ( $G'$ ) and the loss modulus ( $G''$ ) of gels. As shown in Figure 3, it is obvious that  $G'$  is always higher than  $G''$  for either MIG1 or MIG2 over the range of 0.02–100 rad·s<sup>-1</sup>. Both  $G'$  and  $G''$  are slightly sensitive to angular frequency and the average  $G'$  was about twelve times higher than  $G''$  in the tested range. These values of mechanical properties were tested 15 d after synthesis of metal-IDA gels. MIG1 possesses a rela-

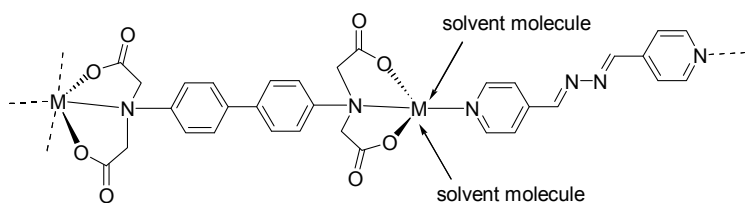


**Figure 2** Assumed structure of metal-IDA gel.

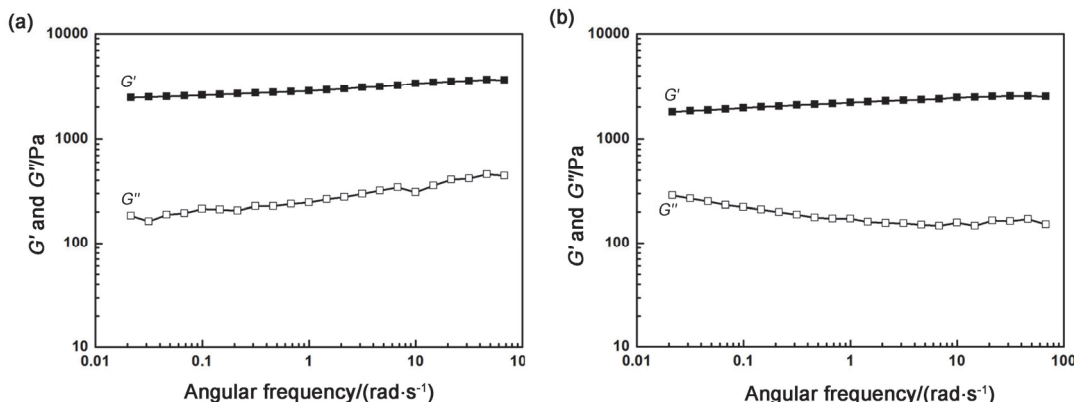


**Figure 3** Dynamic rheology behaviors of MIG1 (a) and MIG2 (b).

tively high storage modulus ( $2.6 \text{ kPa} < G' < 4 \text{ kPa}$ ) than MIG2 ( $1.9 \text{ kPa} < G' < 2.7 \text{ kPa}$ ), indicating the MIG1 has a higher degree of cross-linking. The reason may be that chromium is a heavy metal that has a stronger coordination ability compared to aluminum. The results indicate that the MIGs have markedly elastic rather than viscous characteristics when applying dynamic load and the metal-IDA gels have permanent network structures.

In order to further explore the network structures of MIGs, aerogels were prepared by freeze-drying the prepared gels. The morphology and microstructure of the MIG1 and MIG2 aerogels were observed by SEM and TEM measurements (Figures 4 and S8, Supporting Information). The SEM images (Figures 4a and S8a, Supporting Information) show sponge-like and 3D porous network structures of MIG1 and MIG2. The TEM images (Figures 4b and S8b, Supporting Information) further reveal that aerogels are irregularly interconnected to span large void space and sustain the gel matrix and the particles were amorphous with no long-ranged order. The X-ray powder diffraction patterns (Figure S9, Supporting Information) with weak and broad signals indicate the amorphous nature of the aerogels.

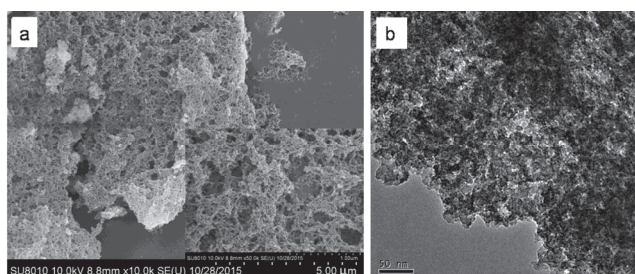


**Figure 4** SEM (a) and TEM (b) micrographs of MIG1 aerogel.

The chemical compositions of MIG1 and MIG2 aerogels were analyzed by X-ray photoelectron spectroscopy (XPS) measurement as shown in Figures 5 and S10 (Supporting Information). In the XPS survey spectrum of MIG1 aerogel (Figure S10a, Supporting Information), the carbon-, oxygen-, nitrogen-, and chromium-related peaks are detected, which contains C, O, N, and Cr of 55.2, 31.4, 7.8, and 5.5 at%, respectively. The

presence of  $\text{Cr}^{3+}$  was evidenced by a signal at 578 eV in the Cr 2p<sub>3/2</sub> region, and a signal at 587 eV in the Cr 2p<sub>1/2</sub> region,<sup>[29]</sup> respectively (Figure 5a). The high-resolution spectrum shows a broad peak of N 1s, indicating the presence of C=N at 399.5 eV<sup>[15]</sup> (Figure 5b). IR spectra of the aerogels and BP-IDA, 4-bpmb (Figure 6) further confirm the coordination of the carboxylate and pyridine group to metal ions, as evidenced by the shift of the C=O stretching frequency from *ca.* 1721 cm<sup>-1</sup> for the uncoordinated carboxylic acid to 1619 cm<sup>-1</sup>, the C=N stretching frequency<sup>[42]</sup> from *ca.* 1418 cm<sup>-1</sup> for the uncoordinated pyridine to 1384 cm<sup>-1</sup> for the aerogels. The thermal stability of the aerogels was studied by TGA measurement (Figure S11, Supporting Information). The aerogels were heated at a rate of 10 °C•min<sup>-1</sup> to 800 °C in nitrogen atmosphere and showed continuous mass loss from room temperature to 800 °C. For these aerogels, the weight loss (10%) at temperatures below 200 °C may be due to the loss of solvent molecules that exactly chelate metal ions in line with the expectative structure or trapped inside the networks.

Good stability and strength of metal-IDA gels may originate from their excellent porosity of network structures. Nitrogen adsorption-desorption measurements at 77 K were performed to investigate the porous property of MIG1 and MIG2 aerogels. As shown in Figure 7a, both MIG1 and MIG2 aerogels display a combination of type I and II sorption isotherms according to the IUPAC classification. The isotherms exhibit a high gas uptake at the relative pressure ( $p/p_0$ ) less than 0.02, a flat course at the middle relative pressure, and sharp gas adsorption at the high relative pressure, which indicate a significant microporosity and macroporosity in the MIG aerogels. The BET specific surface area results are found to be 760 and 430 m<sup>2</sup>•g<sup>-1</sup> for MIG1 and MIG2 aerogels, respectively. Owing to their flexible structure in their networks, MIGs exhibit relatively lower specific surface area compared with other metal-organic gel counterparts reported.<sup>[43,44]</sup> The micropore specific surface area using the *t*-plot method is 90 and 50 m<sup>2</sup>•g<sup>-1</sup>, while the total pore volume at  $p/p_0=0.99$  is up to 2.5 and 1.7 cm<sup>3</sup>•g<sup>-1</sup>. Figure 7b shows the pore size distribution (PSD) profiles of MIG1 and MIG2 aerogels based on nonlocal

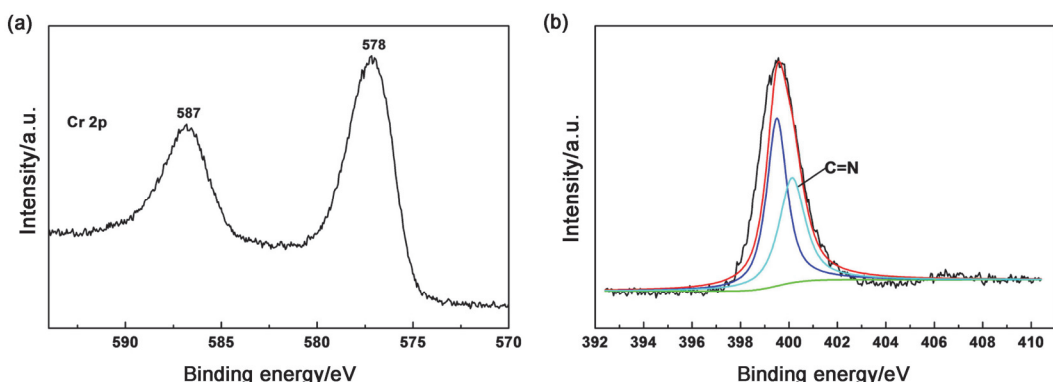


**Figure 5** X-ray photoelectron spectroscopy (XPS) spectra of Cr 2p (a) and resolved N 1s (b).

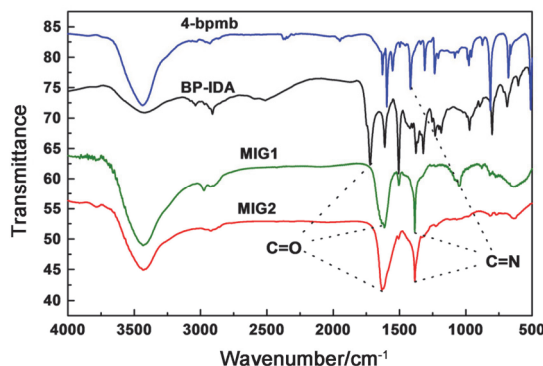


**Figure 6** IR spectra of 4-bpmb, BP-IDA, MIG1 and MIG2 aerogels.

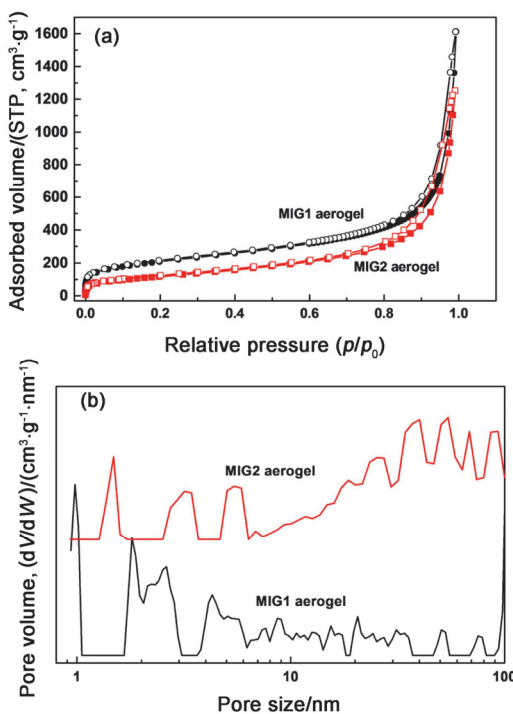


**Figure 7** Nitrogen sorption isotherms of MIG1 and MIG2 aerogels at 77 K (a) and pore size distribution profiles of MIG1 and MIG2 aerogels calculated by the NLDFT approach (b).

density functional theory (NLDFT). The steep peaks are located at 0.98–1.81 nm in the micropore area, and a great amount of mesopores and macropores can be found from 2–100 nm. The results reveal that the obtained aerogels possess the pore size distributions from micro- to macro-regions. Stable network structures of these gels make them become porous materials and have a potential ability to possess gas selective adsorption performance.

## Conclusions

In summary, a novel aromatic multi-carboxylate compound BP-IDA is designed and synthesized by an easy method, and two new types of porous metal-organic gels MIG1 and MIG2 have been easily obtained via solvothermal process. The reaction conditions

to produce MIGs were optimized by varying metal-ligand ratio, temperature, and concentration. Rheology measurement confirms the rigidity and elastic behavior of metal-IDA gels, and their sponge-like morphologies were investigated by SEM and TEM observations. In order to evaluate the 3D network structure of MIGs, aerogels were acquired by freeze-drying the gels. Nitrogen sorption isotherm measurements reveal that MIG aerogels possess high specific surface area and exhibit obvious pore size distribution in micropore and macropore regions. These characteristics make MIGs have a wide range of potential applications including separation, catalysis, and drug delivery.

## Acknowledgement

The financial support of the National Natural Science Foundation of China (Nos. 21374024, 21301119, 21304022, and 21574032) is acknowledged.

## References

- [1] Yang, Q.; Liu, D.; Zhong, C.; Li, J.-R. *Chem. Rev.* **2013**, *113*, 8261.
- [2] Pei, X.; Chen, Y.; Li, S.; Zhang, S.; Feng, X.; Zhou, J.; Wang, B. *Chin. J. Chem.* **2016**, *34*, 157.
- [3] Lu, K.; He, C.; Lin, W. *J. Am. Chem. Soc.* **2015**, *137*, 7600.
- [4] Mondloch, J. E.; Bury, W.; David, F.-J.; Kwon, S.; DeMarco, E. J.; Weston, M. H.; Sarjeant, A. A.; Nguyen, S. T.; Stair, P. C.; Snurr, R. Q.; Farha, O. K.; Hupp, J. T. *J. Am. Chem. Soc.* **2013**, *135*, 10294.
- [5] Zhang, J.; Su, C.-Y. *Coord. Chem. Rev.* **2013**, *257*, 1373.
- [6] Xue, C.; Zhong, C. *Chin. J. Chem.* **2009**, *27*, 472.
- [7] Jung, J. H.; Lee, J. H.; Silverman, J. R.; John, G. *Chem. Soc. Rev.* **2013**, *42*, 924.
- [8] Tam, A. Y.-Y.; Yam, V. W.-W. *Chem. Soc. Rev.* **2013**, *42*, 1540.
- [9] Abdallah, B. D. J.; Weiss, R. G. *Adv. Mater.* **2000**, *12*, 1237.
- [10] Kumar, D. K.; Jose, D. A.; Das, A.; Dastidar, P. *Chem. Commun.* **2005**, 4059.
- [11] Li, H.; Tan, X.; Zhang, J. *Chin. J. Chem.* **2015**, *33*, 141.
- [12] Chen, P.; Li, Q.; Grindley, S.; Niels, H.-A. *J. Am. Chem. Soc.* **2015**, *137*, 11590.
- [13] Xiao, B.; Zhang, Q.; Huang, C.; Li, Y. *RSC Adv.* **2015**, *5*, 2857.
- [14] Wei, S.-C.; Pan, M.; Li, K.; Wang, S.; Zhang, J.; Su, C.-Y. *Adv. Mater.* **2014**, *26*, 2072.
- [15] Dhara, B.; Patra, P. P.; Jha, P. K.; Jadhav, S. V.; Kumar, G. V. P.; Ballav, N. *J. Phys. Chem. C* **2014**, *118*, 19287.
- [16] Yang, Q.; Tan, X.; Wang, S.; Zhang, J.; Chen, L.; Zhang, J.-P. *Microporous Mesoporous Mater.* **2014**, *187*, 108.
- [17] Cui, L.; Wu, J.; Ju, H. *ACS Appl. Mater. Interfaces* **2014**, *6*, 16210.
- [18] Lee, H.; Lee, J. H.; Kang, S.; Lee, J. Y.; John, G.; Jung, J. H. *Chem. Commun.* **2011**, *47*, 2937.
- [19] Piepenbrock, M. M.; Clarke, N.; Steed, J. W. *Soft Matter* **2011**, *7*, 2412.
- [20] Afrasiabi, R.; Kraatz, H.-B. *Chem. Eur. J.* **2015**, *21*, 7695.
- [21] Blake, K. M.; Johnston, L. L.; Braverman, M. A.; Nettleman, J. H.; Sposato, L. K.; LaDuca, R. L. *Inorg. Chim. Acta* **2010**, *363*, 2233.
- [22] Parshamoni, S.; Sanda, S.; Jena, H. S.; Tomar, K.; Konar, S. *Cryst. Growth Des.* **2014**, *14*, 2022.
- [23] Dey, R.; Halder, R.; Maji, T. K.; Ghoshal, D. *Cryst. Growth Des.* **2011**, *11*, 3905.
- [24] Tang, L.; Bai, L.; Duan, Y.; Xia, W.; Dong, W.; Li, D. Z. *Anorg. Allg. Chem.* **2014**, *640*, 2268.
- [25] Ni, L.-B.; Zhang, R.-H.; Liu, Q.-X.; Xia, W.-S.; Wang, H.; Zhou, Z.-H. *J. Solid State Chem.* **2009**, *182*, 2698.
- [26] Zhang, J.; Xue, Y.-S.; Li, Y.-Z.; Du, H.-B.; You, X.-Z.

- CrystEngComm* **2012**, *14*, 8215.
- [27] Karmakar, A.; Goldberg, I. *CrystEngComm* **2011**, *13*, 339.
- [28] Zhan, C.; Zou, C.; Kong, G.-Q.; Wu, C.-D. *Cryst. Growth Des.* **2013**, *13*, 1429.
- [29] Eubank, J. F.; Mouttaki, H.; Cairns, A. J.; Belmabkhout, Y.; Wojtas, L.; Luebke, R.; Alkordi, M.; Eddaoudi, M. *J. Am. Chem. Soc.* **2011**, *133*, 14204.
- [30] Park, I.-H.; Medishetty, R.; Lee, H.-H.; Herring, T. S.; Ding, J.; Lee, S. S.; Vittal, J. J. *Cryst. Growth Des.* **2015**, *15*, 4156.
- [31] Xiang, S.; Li, L.; Zhang, J.; Xin, T.; Cui, H.; Shi, J.; Hu, Y.; Chen, L.; Su, C.-Y.; James, S. L. *J. Mater. Chem.* **2012**, *22*, 1862.
- [32] Kennedy, A. R.; Brown, K. G.; Graham, D.; Kirkhouse, J. B.; Kittner, M.; Major, C.; McHugh, C. J.; Murdoch, P.; Smith, W. E. *New J. Chem.* **2005**, *29*, 826.
- [33] Meng, X.-M.; Zhu, M.-Z.; Liu, L.; Guo, Q.-X. *Tetrahedron Lett.* **2006**, *47*, 1559.
- [34] Ngwendson, J. N.; Amiot, C. L.; Srivastavab, D. K.; Banerjee, A. *Tetrahedron Lett.* **2006**, *47*, 2327.
- [35] Sun, F.; Zhang, G.; Zhang, D.; Xue, L.; Jiang, H. *Org. Lett.* **2011**, *13*, 6378.
- [36] Sui, Z.; Zhang, X.; Lei, Y.; Luo, Y. *Carbon* **2011**, *49*, 4314.
- [37] Yang, T.-H.; Silva, A. R.; Fuc, L.; Shi, F.-N. *Dalton Trans.* **2015**, *44*, 13745.
- [38] Siddiqi, Z. A.; Shahid, M.; Khalid, M.; Kumar, S. *J. Med. Chem.* **2009**, *44*, 2517.
- [39] Ma, X.; Zhang, J.; Tang, N.; Wu, J. *Dalton Trans.* **2014**, *43*, 17236.
- [40] Lin, Q.; Yang, Q.-P.; Sun, B.; Fu, Y.-P.; Zhu, X.; Wei, T.-B.; Zhang, Y.-M. *Soft Matter* **2014**, *10*, 8427.
- [41] Yao, H.; You, X.-M.; Lin, Q.; Li, J.-J.; Guo, Y.; Wei, T.-B.; Zhang, Y.-M. *Chin. Chem. Lett.* **2013**, *24*, 703.
- [42] Dong, Z.; Liu, J.; Yuan, W.; Yi, Y.; Zhao, L. *Chem. Eng. J.* **2014**, *283*, 504.
- [43] Li, L.; Xiang, S.; Cao, S.; Zhang, J.; Ouyang, G.; Chen, L.; Su, C. *Nat. Commun.* **2013**, *4*, 1774.
- [44] Xia, W.; Zhang, X.; Xu, L.; Wang, Y.; Lin, J.; Zou, R. *RSC Adv.* **2013**, *3*, 11007.

(Cheng, F.)